HOKKAIDO UNIVERSITY

Title	Sulfate ion in raw water affects performance of high-basicity PACl coagulants produced by Al(OH)₃ dissolution and base-titration : removal of SPAC particles by coagulation-flocculation, sedimentation, and sand filtration
Author(s)	Chen, Yize; Nakazawa, Yoshifumi; Matsui, Yoshihiko et al.
Citation	Water research, 183, 116093 https://doi.org/10.1016/j.watres.2020.116093
Issue Date	2020-09-15
Doc URL	https://hdl.handle.net/2115/86771
Rights	© 2020. This manuscript version is made available under the CC-BY-NC-ND 4.0 license http://creativecommons.org/licenses/by-nc-nd/4.0/
Rights(URL)	https://creativecommons.org/licenses/by-nc-nd/4.0/
Type	journal article
File Information	Sulfate ion in raw watter affects HUSCAP.pdf

1

Sulfate ion in raw water affects performance of high-basicity PACl

coagulants produced by Al(OH)$_3$ dissolution and base-titration: removal

of SPAC particles by coagulation-flocculation, sedimentation, and sand

filtration

6

Yize Chen [a], Yoshifumi Nakazawa [a], Yoshihiko Matsui [b, *], Nobutaka Shirasaki [b], Taku
Matsushita [b]

9

[a] Graduate School of Engineering, Hokkaido University.

   N13W8 Sapporo 060-8628 Japan

[b] Faculty of Engineering, Hokkaido University

   N13W8 Sapporo 060-8628 Japan

14

* Corresponding author. Phone: +81-11-706-7280.

  E-mail address: matsui@eng.hokudai.ac.jp (Y. Matsui)

17

18

19

20   **ABSTRACT**

21

22   Many PACl (poly-aluminum chloride) coagulants with different characteristics have been

23   trial-produced in laboratories and commercially produced, but the selection of a proper

24   PACl still requires empirical information and field testing. Even PACls with the same

25   property sometimes show different coagulation performances. In this study, we compared

26   PACls produced by $AlCl_3$-titration and $Al(OH)_3$-dissolution on their performance during

27   coagulation-flocculation, sedimentation, and sand filtration (CSF) processes. The

28   removal targets were particles of superfine powdered activated carbon (SPAC), which are

29   used for efficient adsorptive removal of micropollutants, but strict removal of SPAC is

30   required because of the high risk of their leakage after CSF. PACls of high-basicity

31   produced by $AlCl_3$-titration and $Al(OH)_3$-dissolution were the same in terms of the ferron

32   assay and colloid charge, but their performance in CSF were completely different. High-

33   basicity $Al(OH)_3$-dissolution PACls formed large floc particles and yielded very few

34   remaining SPAC particles in the filtrate, whereas high-basicity $AlCl_3$-titration PACls did

35   not form large floc particles. High-basicity PACls produced by $Al(OH)_3$-dissolution were

36   superior to low-basicity PACl in lowering remaining SPAC particles by the same method

37   because of their high charge neutralization capacity, although their floc formation ability

38   was similar or slightly inferior. However, high-basicity $Al(OH)_3$-dissolution PACl was

39   inferior when the sulfate ion concentration in the raw water was low. Sulfate ions were

40   required in the raw water for high-basicity PACls to be effective in floc formation. In

41   particular, very high sulfate concentrations were required for high-basicity $AlCl_3$-titration

42   PACls. The rate of hydrolysis, which is related to the polymerization of aluminum species,

43   is a key property, besides charge neutralization capacity, for proper coagulation, including

44   formation of large floc particles. The aluminum species in the high-basicity PACls, in

45   particular that produced by $AlCl_3$-titration, was resistant to hydrolysis, but sulfate ions in

46   raw water accelerated the rate of hydrolysis and thereby facilitated floc formation.

47   Normal-basicity $Al(OH)_3$-dissolution PACl was hydrolysis-prone, even without sulfate

48   ions. Aluminum species in the high-basicity $AlCl_3$-titration PACl were mostly those with

49   a molecular weight (MW) of 1–10 kDa, whereas those of high-basicity $Al(OH)_3$-

50   dissolution PACls were mostly characterized by a MW >10 kDa. Normal-basicity

51    $Al(OH)_3$-dissolution PACl was the least polymerized and contained monomeric species.

52

53   *Keywords:* hydrolysis; ferron; basicity; floc; PACl

54

55

56

1. Introduction

With the recent development of milling technology, it is possible to produce superfine powdered activated carbon (SPAC) by micro-milling conventionally sized PAC (powdered activated carbon) to a mean diameter of ~1 μm (Matsui et al., 2004, 2013b). The larger adsorption capacity and faster adsorption kinetics of SPAC compared with PAC lead to superior adsorptive removal of organic pollutants from water by SPAC (Ando et al., 2010; Bonvin et al., 2016; Matsui et al., 2015, 2012; Partlan et al., 2016). These advantages of SPAC have led to the expectation that it will be used in water and wastewater treatment (Bonvin et al., 2016). However, there is a concern that the risk of leakage from the treatment process may be higher for SPAC than for conventionally sized PAC. The application of high-basicity (basicity 70%) PACl (polyaluminum chloride) coagulant instead of normal-basicity PACl coagulant has been proposed as an effective way to minimize the loss of SPAC particles during the CSF (coagulation-flocculation, sedimentation, and sand filtration) process, but not all types of high-basicity PACls are effective coagulants (Nakazawa et al., 2018a). The reason is not yet clear.

In Japan, the country where PACl was invented, high-basicity PACl is rapidly becoming a popular replacement for normal basicity coagulant (50%) because use of high-basicity PACl results in lower aluminum residuality in treated water and higher removal efficiencies of natural organic matter (NOM). Furthermore, high-basicity PACl has a greater ability to attenuate transmembrane pressure rise when it is applied in coagulation pretreatment before membrane microfiltration, and storage of high-basicity PACl for a long time does not result in aluminum hydroxide precipitation (Kimura et al., 2015, 2013). However, high-basicity PACl sometimes fails to outperform normal-basicity

81   PACl (personal communication, Taki Chemical Co., Ltd., 2019).

82   High-basicity and normal-basicity PACls are commercially produced by the $Al(OH)_3$-

83   dissolution method. However, PACls produced by base-titration methods have been

84   intensively studied in laboratory coagulation experiments, and satisfactory coagulation

85   performance has been reported based on the residual turbidity after sedimentation (Chu

86   et al., 2008; Gao and Yue, 2005). However, Nakazawa et al. (2018a) have reported that

87   high-basicity PACls produced by $Al(OH)_3$-dissolution and by $AlCl_3$-titration perform

88   very differently, although they are identical in terms of aluminum species based on the

89   ferron assay (Wang et al., 2002). The former was very effective, but the latter was

90   ineffective in forming large floc particles. Use of the latter resulted in a high concentration

91   of residual SPAC particles in treated water. Overall, the evaluations of base-titration

92   PACls have not been consistent. Even when water has been treated with several types of

93   $Al(OH)_3$-dissolution PACl coagulants, the performance of the PACls has generally been

94   specific to the raw water. The mechanisms responsible for this specificity have not been

95   fully investigated and are not yet clearly understood.

96   One possibility is that PACl performance depends on the concentrations of inorganic

97   ions as well as the concentrations of suspended particles and NOM in the raw water. The

98   alkalinity of the raw water is believed to affect the efficiency with which turbidity and

99   particles are removed by PACl coagulation because the aluminum ions in the PACl must

100 undergo hydrolysis to become species that can effect coagulation, and the hydrolysis

101 allows protons to react with alkalinity (Ye et al., 2007). Multivalent ions such as the

102 sulfate ion, which is commonly found in raw water, are also thought to influence

103 coagulation because they destabilize positively charged aluminum polynuclear species

104 (Letterman and Yiacoumi, 2010). However, the effects of sulfate ions have not been

105   sufficiently studied. Sricharoenchaikit and Letterman (1987) have reported that sulfate

106   ions influence the flocculation kinetics of a polystyrene suspension destabilized by

107   aluminum nitrate. Wang et al. (2002) focused on the effect of the sulfate ion in $AlCl_3$-

108   titration PACl coagulants but not on the sulfate ions in raw water.

109   Moreover, most of the foregoing studies of PACl coagulation have used PACls

110   prepared by the $AlCl_3$-titration method, but the characteristics and coagulation

111   performances of PACls produced by the $Al(OH)_3$-dissolution method, which is quite

112   popular in PACl-production industries, have seldom been studied. Experimental results

113   of a series of CSF processes, rather than of jar tests, are still not enough for PACl

114   coagulants.

115   In this study, we measured the concentrations of residual SPAC particles after the CSF

116   process as well as the flocculation-sedimentation characteristics of SPAC particles with

117   the following two objectives. The first objective was to investigate the coagulation

118   characteristics of high-basicity PACls produced by two methods: $Al(OH)_3$-dissolution and

119     $AlCl_3$-titration. The second objective was to investigate the effects of sulfate ions in the

120   raw water.

121

122   **2. Materials & methods**

123

124   *2.1 Coagulants*

125   Three kinds of PACls were used in this study. Among them, PACl-70d (basicity 70%)

126   and PACl-50d (basicity 50%) ("d" represents "dissolution") are commercially available

127   PACls and were provided by Taki Chemical Co., Ltd. (Hyogo. Japan), which produced

128   them by dissolving $Al(OH)_3$ in HCl and H_2SO_4 [as described in Sato and Matsuda (2009)].

129   Briefly, a mixture of $AlCl_3$, $Al_2(SO_4)_3$, and $Al(OH)_3$ was heated to obtain a solution with

130   a basicity of 50% ($Al(OH)_3$-dissolution method). The basicity was then raised to 70% at

131   <85 °C by adding a solution of sodium carbonate. The third kind of PACl used, PACl-70t

132   ("t" represents "titration"), was produced in the authors' laboratory by titrating a NaOH

133   solution into an $AlCl_3$ solution. The procedure, which is called the $AlCl_3$-titration method,

134   consists of the following steps. A NaOH solution (1 mol/L; Kanto Chemical Co., Inc.,

135   Tokyo, Japan) is diluted with ultrapure water (Milli-Q water) produced by an ultrapure

136   lab water system (Milli-Q Advantage; Merck KGaA, Darmstadt, Germany) to a

137   concentration of 0.26 mol/L. Then, $AlCl_3 \cdot 6H_2O$ and $Al_2(SO_4)_3 \cdot 16H_2O$ (FUJIFILM Wako

138   Pure Chemical Corporation) are dissolved to obtain 80 mL of a 0.5-M Al solution. A pump

139   and tubes are prepared for titrating the NaOH solution with the Al solution. After the

140   NaOH solution and Al solution are heated to 50–60 °C and 85–90 °C, respectively, the

141   titration is started. The flow rate of the NaOH solution is set at 4 mL/min to avoid the

142   appearance of a precipitate during the titration. After the titration is finished, the resultant

143   solution is preserved in a refrigerator at 4 °C for one night and then heated at 90–95 °C

144   for 3 hours. After the temperature has returned to room temperature, the solution is

145   preserved at 4 °C until the time of the experiment. Table 1S (SI) lists the basic properties

146   of the PACl coagulants. During the experiment, PACls from the stock were first diluted

147   to 0.1 mol-Al/L using Milli-Q water. The dosage of PACl coagulant was 2.5 mg-Al/L

148   unless otherwise noted.

149

150   *2.2 Superfine powdered activated carbon (SPAC)*

151   A commercially available wood-based PAC (Taiko W) was obtained from Futamura

152   Chemical Co., Ltd. (Nagoya, Japan) and was milled with a bead mill (LMZ015; Ashizawa

153   Finetech, Ltd., Chiba, Japan) to produce a SPAC. The details of the procedure are

154   described elsewhere (Pan et al., 2017).

155

156   *2.3 Water*

157   Three kinds of water (C, E, and J series) were prepared (Table 1). Water of the C series

158   was prepared from natural water (designated as C0) that was sampled from the Chibaberi

159   River (Rumoi City, Hokkaido, Japan). Water C0 was diluted with pure water (Elix water,

160   Elix Advantage; Merck KGaA, Darmstadt, Germany), and its ion concentrations were

161   adjusted by adding $NaHCO_3$ or Na_2SO_4 (FUJIFILM Wako Pure Chemical Corporation)

162   to prepare Waters C1 and C2. Waters of the E series (E1–7) were ionic waters prepared

163   by adding $MgSO_4$, $CaCl_2$, HNO_3, KOH, Na_2SO_4, and $NaHCO_3$ to Elix water. There were

164   two waters in the J series: water sampled from the Joganji River (Toyama, Japan) and the

165   same water adjusted by addition of Na_2SO_4. Alkalinity, which might affect the coagulation,

166   was adjusted at each constant for C2–3, E1–7, and J1–2 waters. These waters were stored

167   at 4 °C. The waters were ready for a PACl hydrolysis test after their temperatures had

168   returned to room temperature (~20 °C). The waters were ready for CSF experiments after

169   their temperatures had returned to room temperature and SPAC (the target for removal)

170   had been added at a concentration 2 mg/L. Concentrations of ions in the water were

171   measured by ion chromatography (ICS-1000 and ICS-1100; Thermo Scientific, Bremen,

172   Germany). The alkalinity was measured by titrating the water with 0.01 M H_2SO_4. For

173   the measurement of dissolved organic carbon (DOC), the water sample was filtered

174   through a membrane filter (0.45-μm pore size; Toyo Roshi Kaisha, Ltd., Tokyo, Japan),

175   and the DOC was then measured with a TOC analyzer (TOC900; GE Analytical

176   Instruments, Inc., Boulder, CO, USA).

177

2.4 Characterization of PACl coagulants

The ferron assay was conducted with the 3 PACls. Immediately after being diluted with Milli-Q water to a concentration of 0.1 mol-Al/L, the PACls were added to the ferron reagent (8-hydroxy-7-indo-5-quinoline sulfonic acid; FUJIFILM Wako Pure Chemical Corporation) to initiate the reaction. The absorbance at 366 nm was then measured using an ultraviolet light meter (UV-1800; Shimadzu, Kyoto, Japan). Dilution of the PACls was acceptable because dilution has little effect on the distribution of ferron (Kimura et al., 2013; Wang et al., 2002). The aluminum species in the PACl were divided based on their reaction time with the ferron reagent into Ala (monomeric species, within 30 s), Alb (polymeric species, from 30 s to 120 min), and Alc (colloidal species, did not react within 120 min) (Wang et al., 2004; Yan et al., 2007).

The colloid charges of the PACls were measured via colloid titration. A PACl was diluted with Milli-Q water into 0.1 mol-Al/L and was titrated with a potassium polyvinyl sulfate titration solution (N/400, for colloidal titration; FUJIFILM Wako Pure Chemical Corporation) using an automatic titrator (COM-555; Hiranuma Sangyo Co., Inc., Ibaraki, Japan) (Matsui et al., 2017).

For the ESI-MS analyses, PACls were diluted to a concentration of 0.1 mol-Al/L and introduced into an Orbitrap LC-MS system (Exactive; Thermo scientific, Bremen, Germany) under the following conditions: scan range *m/z* 200–2000; spray voltage 3.0 kV; capillary temperature 300 °C; capillary voltage 32.5 V; heater temperature 250 °C. Peaks and the possible formulas of aluminum species were calculated by Xcalibur 2.2 (Thermo Fisher Scientific).

^{27}Al-NMR analysis was conducted with a JNM-ECA Series FT NMR (ECA 600;

201 JEOL Ltd., Tokyo, Japan). NaAl(OH)$_4$ (FUJIFILM Wako Pure Chemical Corporation)

202 solution (0.01 mol-Al/L) was used as the internal standard. AlCl$_3$ (FUJIFILM Wako Pure

203 Chemical Corporation) solution (0.1 mol-Al/L) was used as the reference material.

204 Parameters for the measurement were as follows: field strength, 14.09 T; frequency,

205 78247 Hz; resonance frequency, 156.39 MHz; number of scans, 8000; temperature 70 °C.

206 The data and peaks were processed with the data-processing software provided with

207 Nakamura (2009).

208 　　　The molecular weight (MW) distributions of aluminum species were measured by

209 using membrane filters with nominal MW cutoffs of 1 and 10 kDa (regenerated cellulose

210 membrane, Ultracel PL; Merck KGaA, Darmstadt, Germany). The membrane filters were

211 set in 50-mL stirred cells (Amicon 8050 series; Merck KGaA, Darmstadt, Germany).

212 Coagulants with concentrations higher than 0.1 mol-Al/L were diluted to 0.1 mol-Al/L

213 using Milli-Q water in the stirred cell. The filtration was then started by applying 0.5-

214 MPa pressure at 30 s after dilution. The filtration continued until 2 mL of filtrate had been

215 collected from the 50-mL sample. The aluminum concentrations in the filtrates were

216 measured with an inductively coupled plasma mass spectrometer (ICPMS, 7700x; Agilent

217 Technologies, Inc., Santa Clara, CA, USA).

218 　　　The following procedure was used to determine the rate of hydrolysis of the aluminum

219 species in PACl. E-series water was placed in a 1-L rectangular plastic beaker. HCl or

220 NaOH (0.1N) was added to bring the final pH to 7, and then PACl was added so that the

221 concentration of aluminum was 2.5 mg/L. The solution was mixed at a G value (velocity

222 gradient) of 600 s^{-1} for 40 s and then at a G value of 50 s^{-1} for 80 s. Ten-milliliter samples

223 of water were taken at times of 15 s, 30 s, 60 s, and 120 s after the PACl injection. A

224 portion of the sample was immediately filtered through a polytetrafluoroethylene (PTFE)

225   membrane (Φ47 mm; Merck KGaA, Darmstadt, Germany) with a pore size of 0.1, 1, or

226   10 μm. A PTFE membrane was used in this experiment because PTFE membranes have

227   been reported to have the lowest tendency to adsorb aluminum (Matsui et al., 2013a). The

228   Al concentration in the filtrate was measured by ICPMS.

229

230   *2.5 Coagulation-flocculation, sedimentation, and rapid sand filtration (CSF) experiment*

231   CSF experiments were used to evaluate the coagulation performances of the PACls.

232   Four liters of raw water were placed in a rectangular plastic beaker. A predetermined

233   volume of HCl or NaOH (0.1N) was added to the water to adjust the coagulation pH to

234   7.0. After 30 min of mixing, PACl was added. Rapid mixing conducted at a G value of

235   600 s^{-1} for 40 s was followed by three stages of slow mixing at G values (in chronological

236   order) of 50 s^{-1} for 170 s, 20 s^{-1} for 170 s, and 10 s^{-1} for 320 s, respectively. The total GT

237   value for the rapid and slow mixing was 39,100. After mixing, the water was allowed to

238   stand for 1 hour for sedimentation. The supernatant was then transferred at a constant rate

239   to the sand-filtration column for sand filtration. Sand filtration was conducted at a rate of

240   90-m/d with a 50-cm–deep column containing sand (effective diameter, 0.6 mm;

241   uniformity, 1.3). Filtrate was collected from 13 to 40 min after the start of filtration. After

242   the filtration was finished, the sand filter was backwashed with tap water and then forward

243   washed with Milli-Q water.

244   The Zeta potentials of the water before coagulation, the water after rapid mixing, and

245   the supernatant were measured with a Zeta potential meter (Zetasizer Nano ZS; Malvern

246   Panalytical Ltd., Almelo, Netherlands) using a dip cell. The turbidity of the water before

247   coagulation, the supernatant, and the sand filtrate were measured with a turbidity meter

248   (2100Q portable turbidimeter; Hach Company, Loveland, CO, USA). Formation of floc

249   particles was evaluated based on pictures of the beaker taken with a DSLR (digital single

250   lens reflex) camera (EOS 60D; Canon Ltd., Tokyo, Japan) at the end of rapid mixing and

251   during slow mixing.

252

253   *2.6. Membrane filtration and image analysis*

254   The carbon particles that remained in the sand filtrate were enumerated via membrane

255   filtration and image analysis. The details of this method have been described by

256   Nakazawa et al. (2018b) but can be briefly described as follows. Sample water was

257   filtered through a membrane filter (pore size 0.1 μm, PTFE, Φ25 mm; Merck KGaA), and

258   then the filter was allowed to dry under natural conditions. Photographs of the filter were

259   taken with a microscope (VHX-2000; Keyence corporation, Osaka, Japan), and the SPAC

260   particles on the photographs were counted with the software built into the microscope.

261

262   **3. Results and discussion**

263

264   *3.1 Characteristics of PACl coagulants*

265   As shown in Fig. 1 (Panel A), the ferron distributions of PACl-70t and PACl-70d were

266   almost the same: Alc species accounted for more than 65% of total aluminum, Alb for

267   ~15%, and Ala for ~20%. Among the three PACls, the percentage of Ala was highest

268   (40%) in PACl-50d. The similarity of the charge neutralization abilities of PACl-70t and

269   PACl-70d (Fig. 1 (Panel B)) reflected the similarities of their ferron distributions. The

270   fact that the charge neutralization ability was smaller for PACl-50d than for PACl-70t and

271   PACl-70d reflected the lower percentage in PACl-50d of Alc + Alb (aluminum colloid

272   and polymer), which are generally regarded as the aluminum species with high charge

273   neutralization capacity (Yan et al., 2008).

274   Marked differences between the three PACls were observed in the MW distributions

275   determined by membrane filtration (Panel C of Fig. 1). PACl-70t contained a relatively

276   large amount of polymerized aluminum species with MWs ranging from 1 to 10 kDa

277   compared with PACl-70d. PACl-50d contained a relatively large amount of aluminum

278   species with low MWs (<1 kDa), which should include Al monomers. Differences were

279   also observed in the ESI-MS spectrum of the three PACls (Fig. 1S, SI), although the

280   formulas of the aluminum species could not be identified.

281   The ^{27}Al-NMR analysis spectra are shown in Fig. 1 (Panel D). The peak at $\delta = 0$ ppm,

282   which is the indication of an Al monomer, was observed for all three PACls, but the fact

283   that it was relatively high in the PACl-50d spectrum compared with the other spectra was

284   consistent with the ferron assay results. A peak at $\delta = 62.5$ ppm is assigned to tetrahedrally

285   coordinated Al in the Keggin Al_{13} structure ($Al(O)_4$) and is related to the presence of an

286   e-Al_{13} polycation (Allouche et al., 2002; Sposito, 1995). This peak was found in all three

287   PACl coagulants and was relatively intense in PACl-70d. The Keggin-type e-Al_{13}

288   polycation is considered to be equivalent to Alb (Chen et al., 2007; Parker and Bertsch,

289   1992; Sposito, 1995), but this equivalence was not supported by the data of the present

290   study: the percentages of Alb were similar in PACl-70d and PACl-70t and relatively small

291   in PACl-50d. The broad resonance observed at $\delta = 10$–12 ppm in PACl-70t and PACl-70d

292   (but not in PACl-50d) was assigned to octahedral aluminum sites [$Al(O)_6$] in oligomers

293   (Casey, 2006; Tang et al., 2015). The larger area and higher intensity of the resonance at

294    $\delta = 10$–12 ppm in PACl-70t versus PACl-70d meant that the amount of $Al(O)_6$ oligomer

295   was higher in PACl-70t than in PACl-70d. The broad resonance at $\delta = \sim 70$ ppm, which is

296   an indication of a Keggin-type δ-Al_{30} polycation, was not observed. PACl-70t and PACl-

297   70d therefore differed with respect to their aluminum species, although the ferron analysis

298   could not distinguish this difference. Finally, the three PACls were different.

299

300   *3.2 Comparison of PACls in CSF experiments*

301   The turbidity and residual SPAC particles during the CSF experiments are shown in

302   Fig. 2 (Panels A and B) and Fig. 2S (SI) for Waters C1 and E4, respectively. Turbidities

303   in the supernatant after sedimentation were very low when either PACl-70d or PACl-50d

304   was used to treat the water, and the turbidities in the sand filtrate after the rapid filtration

305   process reached an even lower level (Fig. 2S, SI). In contrast, use of PACl-70t resulted in

306   a relatively high residual turbidity in the supernatant for Water C1 (Panel A of Fig. 2) and

307   so little turbidity removal after sedimentation for Water E4 (Fig. 2S, SI) that we could not

308   conduct a sand-filtration experiment. Photographs taken during the coagulation-

309   flocculation process are shown in Fig. 2 (Panel C) and Fig. 3S (SI). At the end of slow

310   mixing, the floc size was very small when PACl-70t was used. In contrast, relatively large

311   floc particles were observed for both PACl-50d and PACl-70d. Although the rate of floc

312   formation seemed higher for PACl-50d because of the greater number of micro-floc

313   particles that were clearly observed at the end of rapid mixing, the residual SPAC particles

314   in the sand filtrate when PACl-50d was used was at the same level or higher versus PACl-

315   70d (Fig. 2 (Panel B, Fig. 2S, SI). Although PACl-50d was superior in terms of floc

316   formation, this superiority did not lead to lower numbers of residual SPAC particles in

317   the sand filtrate because of the low charge-neutralization ability of the PACl-50d, which

318   was apparent from the results of the ferron assay and colloid charge (Panels A and B of

319   Fig. 1). Nakazawa et al. (2018a and 2018b) have revealed that particles with un-

320   neutralized charge leak through CSF processes, and high-basicity PACls have a high

321 charge-neutralizing capacity.

322   The performance of PACl-70d and PACl-70t differed to a great extent, although they

323 had nearly the same ferron distribution and colloid charge. The zeta potentials during

324 coagulation using PACl-70d and 70t are shown in Fig. 4S (SI). The higher charge

325 neutralization ability of PACl-70t versus PACl-70d has also been reported by Nakazawa

326 et al. (2018a). The fact that the zeta potential of particles became close to zero after

327 coagulation by PACl-70t meant that charge neutralization progressed well. However, floc

328 formation was much slower with PACl-70t than with PACl-70d. The reason might be the

329 difference in the aluminum species in the PACls, a difference that was seen in the MW

330 distributions and ESI-MS and that was faintly apparent in the ^{27}Al-NMR spectra. The

331 difference, however, was not reflected in the ferron species distribution (Ala, Alb, and

332 Alc) and colloid charge (see section 3.1). Feng et al. (2007) have differentiated Alb

333 (polymeric aluminum species) into two fractions: the faster-reacting polymers and the

334 slower-reacting polymers. However, the main aluminum species in PACl-70d and PACl-

335 70t was Alc (colloid aluminum species), not Alb. The large difference in coagulation

336 performance between PACl-70d and PACl-70t may therefore not be attributable to the

337 difference in the polymeric aluminum species (Alb). The colloid aluminum species (Alc)

338 may include a variety of species with very different reaction rates. Such species

339 differences were observed in the MW distributions and ESI-MS.

340   Aluminum coagulants, including PACls, are hydrolyzing aluminum salt coagulants.

341 The aluminum species in PACl react with alkalinity after it is dosed to water, and the

342 unstable aluminum hydroxide that is finally formed plays an important role in sweep

343 coagulation (Letterman and Yiacoumi, 2010). In this study, we evaluated the speed of

344 aluminum hydrolysis by measuring the concentrations of aluminum after filtration

345 through membranes of different pore sizes (0.1, 1, and 10 μm, Fig. 3). The rapid

346 hydrolysis of PACl-70d and PACl-50d resulted in the most large (>10 μm) Al particles

347 within 15 s after the PACl was injected into the water. The PACl-70t hydrolyzed at a much

348 slower rate: more than half of the Al particles were still <10 μm in size 60 s after injection.

349 The very different rates of hydrolysis of PACl-70t and PACl-70d may have reflected

350 differences in the aluminum species that were observed in the MW distributions and ESI-

351 MS. The difference of coagulation performance could not be explained solely on the basis

352 of charge neutralization ability. Hydrolysis, which can be evaluated with a hydrolysis test,

353 also plays an important role in coagulation performance.

354

355 *3.3 Effect of sulfate ion in water*

356 *3.3.1 Effect of sulfate ion on CSF performance.*

357 The sulfate ion in PACl is known to change the characteristics of the PACl (Nakazawa

358 et al., 2018a). However, PACl-70t and PACl-70d had the same sulfate ion content, and

359 therefore the sulfate ions in the PACls could not have caused a large difference in their

360 coagulation performance. We then focused on the sulfate ions in the raw water. The effect

361 of the sulfate ions was first investigated by using adjusted natural waters (C1 and C2)

362 with different sulfate concentrations. There was no obvious difference in turbidity and

363 removal of SPAC particles between sulfate concentrations of 15.9 mg/L and 6.4 mg/L

364 (Fig. 5S, SI). However, the slower rate of formation of floc at 6.4 mg/L than at 15.9 mg/L

365 (Fig. 4) suggested that there was a sulfate effect.

366 We further investigated the effect of sulfate ions by preparing artificial raw waters

367 with various SO_4^{2-} concentration (E1–7 in Table 1). Fig. 5 shows the rates of turbidity

368 removal by PACl-70t, PACl-70d, and PACl-50d. As the concentration of the SO_4^{2-} ion in

369   the raw water decreased, the removal of turbidity by PACl-70t and PACl-70d in

370   sedimentation supernatant decreased dramatically. In the absence of SO_4^{2-}, there was

371   almost no turbidity removal. Compared with PACl-70d and PACl-70t, on the other hand,

372   treatment with PACl-50d resulted in high turbidity removal, regardless of the SO_4^{2-} ion

373   concentration in the water. Even when the SO_4^{2-} concentration was zero, PACl-50d

374   produced supernatant with a low residual turbidity that was comparable to the turbidity

375   attained with 15.8-mg/L SO_4^{2-}. Photographs of floc formation were consistent with this

376   result (Fig. 6). When PACl-50d was used to treat the water, visible floc particles were

377   observed at the rapid-mixing stage when the water contained SO_4^{2-} at 3.5–15.8 mg/L, and

378   during the first stage of slow mixing, visible floc particles were also observed, even when

379   the water contained no SO_4^{2-} ions (Fig. 8S, SI). For PACl-70d, however, the rate of floc

380   formation slowed as the sulfate ion concentration decreased. When the SO_4^{2-}

381   concentration was 3.5 mg/L, visible floc particles were not formed during the rapid-

382   mixing stage; instead, they were formed only after slow mixing. At a SO_4^{2-} concentration

383   of zero, floc particles were not formed at all. At low sulfate concentrations, the floc

384   formation ability was therefore stronger for PACl-50d than for PACl-70d. PACl-70t

385   required a very high sulfate ion concentration (48.8 mg-SO_4^{2-}/L) for floc formation, but

386   even at such a high sulfate ion concentration, large floc particles did not form.

387   The sulfate ion in PACl is known to enhance the precipitation of aluminum ions in

388   water (De Hek et al., 1978). All commercially available PACls in Japan contain sulfate

389   ions, but JIS (Japanese Industrial Standards) standard JIS K 1475-1996 stipulates that the

390   sulfate ion content of PACl should be lower than 3.5% (Japanese Industrial Standards

391   Committee, 1996). The sulfate contents of PACl-70d and PACl-50d were 2% and 3%,

392   respectively. The unsatisfactory performance of PACl-70d at low SO_4^{2-} concentrations

393   might have resulted from its relatively low sulfate content. In order to test this hypothesis,

394   Fig. 5 was redrawn using the total sulfate ion concentration (sulfate ion concertation in

395   raw water plus sulfate ion added with the PACl) as the independent variable (Fig. 9S, SI).

396   The total sulfate ion concentration did not explain the difference in the coagulation

397   performances of PACl-70d and PACl-50d. Moreover, when PACl-70t and PACl-70d were

398   compared, the requirement for sulfate ions was larger for PACl-70t than for PACl-70d,

399   although the two PACls had the same sulfate content. Nakazawa et al. (2018a) have

400   prepared a set of high-basicity PACl coagulants prepared by the $Al(OH)_3$-dissolution

401   method and have reported that SPAC particle removal ability via PACl coagulation

402   depends little on SO_4^{2-}/Al ratios in the range 0.11–0.15. These results indicate that the

403   requirement of PACl-70d for sulfate ions in raw water is not related to its low sulfate

404   content.

405   A dependence of PACl-70d coagulation on SO_4^{2-} concentrations in water was also

406   observed in the concentrations of residual SPAC particles after CSF (Fig. 7). When SO_4^{2-}

407   concentrations were at a low level of 3.5 mg/L, the residual SPAC particle concentration

408   was quite high, 1790 particles/mL, a concentration that was higher than the concentration

409   of 345 particles/mL achieved with PACl-50d at the same SO_4^{2-} concentration. At a SO_4^{2-}

410   concentration of zero, residual SPAC particles were too numerous to count. Nakazawa et

411   al. (2018a) have observed the superiority of PACl-70d over PACl-50d in reducing residual

412   SPAC particles in water containing SO_4^{2-} at a concentration of 16 mg/L, and this trend

413   was also observed in our study when the SO_4^{2-} concentration exceeded 6.4 mg/L. Our

414   results show, however, that at relatively low SO_4^{2-} concentrations, normal-basicity PACl

415   is superior to high-basicity PACl.

416   The effect of sulfate ions was further confirmed by the experiments using natural

417 water and SO_4^{2-}-adjusted natural water. For PACl-70d, floc did not form during the

418 mixing process (Panel A of Fig. 8), and the result was high residual turbidity in the

419 supernatant (Panel B of Fig. 8). With the increase of the sulfate ion concentration in the

420 water, the coagulation performance improved: formation of large floc particles was

421 observed, and turbidity in the supernatant became satisfactorily low. In contrast, the

422 performance of PACl-50d was fairly good, regardless of whether or not there was an

423 increase of the SO_4^{2-} concentration (Fig. 8). Our results showed that PACl-70d, which is

424 superior in reducing residual SPAC particles after CSF, requires a certain concentration

425 of SO_4^{2-} in the raw water to work efficiently.

426   *3.3.2 Effect of sulfate ion on PACl hydrolysis.*

427   The rates of hydrolysis of PACl-70t, 70d, and 50d at different sulfate concentrations

428 were investigated, and the results are shown in Fig. 9. There was little effect of sulfate

429 ions on the rate of hydrolysis for PACl-50d: the aluminum species in PACl-50 grew larger

430 than 10 μm within 15 s, no matter what the sulfate concentration in the water was. In

431 contrast, the aluminum species in PACl-70d hydrolyzed relatively slowly and grew a little

432 slower at a sulfate concentration of 6.4 mg-SO_4^{2-}/L (Water E3). They barely hydrolyzed

433 without sulfate ions and did not grow larger than 10 μm (Water E1). They grew rapidly at

434 a sulfate concentration of 15.8 mg/L (Waters E4 and E5). Although the concentrations of

435 Na^+ and Mg^{2+} differ in Waters E4 and E5, the rates of the hydrolysis were about the same.

436 The aluminum species in PACl-70t grew very slowly, even at a sulfate concentration of

437 15.8 mg/L. The growth trend of PACl-70t at a sulfate concentration of 48.8 mg/L was

438 similar to that of PACl-70d at a sulfate concentration of 6.4 mg/L. Therefore, the results

439 indicate that sulfate ions are essential for the hydrolysis of PACl-70d and PAC-70t, and

440 they show that PACl-70t requires a much higher concentration of sulfate for its rapid

441   hydrolysis than PACl-70d.

442   The pattern of hydrolysis rates was similar to the trend of coagulation performance,

443   including floc formation and the concentration of residual particles after CSF. On the

444   other hand, charge neutralization capacity, which was evaluated via the ferron assay and

445   colloid charge, did not explain the different coagulation performances of PACl-70d and

446   PAC-70t, as described in the sections 3.1 and 3.2. Hydrolysis rate rather than charge

447   neutralization capacity, therefore determined coagulation performance. Wang et al. (2002)

448   have reported an enhancement of coagulation performance with increasing SO_4^{2-}/Al ratio

449   in PACl and have explained the SO_4^{2-} effect by a charge neutralization mechanism. Our

450   results are new in terms of two points. First, we focused on SO_4^{2-} in raw water, not in

451   PACl. Second, there were different SO_4^{2-} effect on high-basicity PACls of the same

452   sulfate contents (PACl-70d and PACl-70t) but there was no effect on low-basicity PACl

453   (PACl-50d). Sulfate ion in raw water accelerate hydrolysis of aluminum species in high-

454   basicity PACls, but its mechanism is not cleared yet. A possible mechanism is related to

455   ionic strength and double-layer compression. Sulfate ion in raw water may change charge-

456   neutralization capacity of aluminum species formed after PACl is dosed into raw water.

457   These require further study.

458   Moderately polymerized aluminum species with MWs ranging from 1 to 10 kDa were

459   observed in PACl-70t. These moderately polymerized species may have been related to

460   the distinctive hydrolysis of PACl-70t. PACl-70d contained a high percentage of highly

461   polymerized species with MWs >10 kDa. Among the three PACls, PACl-50d had the

462   highest percentage of species with molecular weights <1 kDa, including monomer Al. We

463   hypothesized that the resistance to hydrolysis was strong for moderately polymerized

464   species followed by highly polymerized species. PACl-70t was produced through a high-

465 temperature (90–95 °C) process, whereas PACl-70d was prepared through a low-

466 temperature process (<85 °C). PACl-70t contains more sodium and chloride ions per

467 aluminum than PACl-70d (Table 1S). The production temperature and/or salt content, in

468 addition to basicity, may therefore determine hydrolysis resistance and coagulation ability.

469

470 **4. Conclusion**

471

472 This study comprehensively investigated the difference between PACl-70d ($Al(OH)_3$-

473 dissolution PACl) and PACl-70t ($AlCl_3$-titration PACl) as well as the difference between

474 PACl-70d (high-basicity PACl) and PACl-50d (normal-basicity PACl) in terms of their

475 coagulation ability to form floc particles and to reduce the concentration of SPAC

476 particles in CSF-treated water.

477 The coagulation performance of PACl-70d was superior to that of PACl-70t, although

478 the ferron distribution, colloid charge, and sulfate ion content were the same. Charge

479 neutralization capacities were likewise sufficient for PACl-70t and PACl-70d, but the very

480 low hydrolysis of aluminum species in PACl-70t versus PACl-70d resulted in poor floc

481 formation by the former.

482 PACl-70d was superior to PACl-50d in reducing residual carbon particles after CSF,

483 although the rate of floc particle formation was somewhat slower for PACl-70d than for

484 PACl-50d. The similarities of the residual turbidities after coagulation sedimentation

485 could have been due to the high charge neutralization capacity of PACl-70d. However,

486 sulfate ion was required in raw water for PACl-70d to be effective.

487 When the raw water contained very low concentrations of sulfate ions, the aluminum

488 species in PACl-70d hydrolyzed very slowly and did not form floc particles. In contrast,

489 PACl-50d did not need sulfate ions. Finally, PACl-70d was inferior to PACl-50d when

490 sulfate ion concentrations in raw water were very low.

491   The three PACls were clearly different in terms of their MW distributions and their

492 *m/z* values determined by ESI-MS, but they did not necessarily differ based on the ferron

493 assay. Polymerized aluminum species, in particular those with MWs of 1–10 kDa, might

494 be highly resistant to hydrolysis and may require sulfate ions for hydrolysis and for

495 effective coagulation.

496   Hydrolysis of aluminum species as well as charge neutralization capacity are key

497 determinants of coagulation effectiveness.

498

503

504

505 **References**

506 Allouche, L., Gérardin, C., Loiseau, T., Férey, G., Taulelle, F., 2002. Al30: A Giant

507   Aluminum Polycation. Angew. Chemie Int. Ed. 39, 511–514.

508   https://doi.org/10.1002/(sici)1521-3773(20000204)39:3<511::aid-

509   anie511>3.0.co;2-n

510 Ando, N., Matsui, Y., Kurotobi, R., Nakano, Y., Matsushita, T., Ohno, K., 2010.

511   Comparison of natural organic matter adsorption capacities of super-powdered

512   activated carbon and powdered activated Carbon. Water Res. 44, 4127–4136.

513 https://doi.org/10.1016/j.watres.2010.05.029

514 Bonvin, F., Jost, L., Randin, L., Bonvin, E., Kohn, T., 2016. Super-fine powdered

515 activated carbon (SPAC) for efficient removal of micropollutants from wastewater

516 treatment plant effluent. Water Res. 90, 90–99.

517 https://doi.org/10.1016/j.watres.2015.12.001

518 Casey, W.H., 2006. Large aqueous aluminum hydroxide molecules. Chem. Rev. 106, 1–

519 16. https://doi.org/10.1021/cr040095d

520 Chen, Z., Luan, Z., Fan, J., Zhang, Z., Peng, X., Fan, B., 2007. Effect of thermal

521 treatment on the formation and transformation of Keggin Al13 and Al30 species in

522 hydrolytic polymeric aluminum solutions. Colloids Surfaces A Physicochem. Eng.

523 Asp. 292, 110–118. https://doi.org/10.1016/j.colsurfa.2006.06.005

524 Chu, Y., Gao, B., Yue, Q., Wang, Y., 2008. Investigation of dynamic processing on

525 aluminum floc aggregation: Cyclic shearing recovery and effect of sulfate ion. Sci.

526 China, Ser. B Chem. 51, 386–392. https://doi.org/10.1007/s11426-007-0129-2

527 De Hek, H., Stol, R.J., De Bruyn, P.L., 1978. Hydrolysis-precipitation studies of

528 aluminum(III) solutions. 3. The role of the sulfate ion. J. Colloid Interface Sci. 64,

529 72–89. https://doi.org/10.1016/0021-9797(78)90336-3

530 Feng, C., Tang, H., Wang, D., 2007. Differentiation of hydroxyl-aluminum species at

531 lower OH/Al ratios by combination of 27Al NMR and Ferron assay improved with

532 kinetic resolution. Colloids Surfaces A Physicochem. Eng. Asp. 305, 76–82.

533 https://doi.org/10.1016/j.colsurfa.2007.04.043

534 Gao, B., Yue, Q., 2005. Effect of SO42-/Al3+ratio and O-/Al3+value on the

535 characterization of coagulant poly-aluminum-chloride-sulfate (PACS) and its

536 coagulation performance in water treatment. Chemosphere 61, 579–584.

https://doi.org/10.1016/j.chemosphere.2005.03.013

Japanese Industrial Standards Committee, 1996. Poly aluminum chloride for water

works. URL

https://www.jisc.go.jp/app/jis/general/GnrJISNumberNameSearchList?toGnrJISSta

ndardDetailList

Kimura, M., Matsui, Y., Kondo, K., Ishikawa, T.B., Matsushita, T., Shirasaki, N., 2013.

Minimizing residual aluminum concentration in treated water by tailoring

properties of polyaluminum coagulants. Water Res. 47, 2075–2084.

https://doi.org/10.1016/j.watres.2013.01.037

Kimura, M., Matsui, Y., Saito, S., Takahashi, T., Nakagawa, M., Shirasaki, N.,

Matsushita, T., 2015. Hydraulically irreversible membrane fouling during

coagulation-microfiltration and its control by using high-basicity polyaluminum

chloride. J. Memb. Sci. 477, 115–122.

https://doi.org/10.1016/j.memsci.2014.12.033

Letterman, R.D., Yiacoumi, S., 2010. Coagulation and flocculation, in: Edzwald, J.K.

(Ed.), Water Quality and Treatment A Handbook on Drinking Water. McGrawHill,

pp. 8.1-8.81.

Matsui, Y., Ishikawa, T.B., Kimura, M., Machida, K., Shirasaki, N., Matsushita, T.,

2013a. Aluminum concentrations of sand filter and polymeric membrane filtrates:

A comparative study. Sep. Purif. Technol. 119, 58–65.

https://doi.org/10.1016/j.seppur.2013.09.006

Matsui, Y., Murase, R., Sanogawa, T., Aoki, N., Mima, S., Inoue, T., Matsushita, T.,

2004. Micro-ground powdered activated carbon for effective removal of natural

organic matter during water treatment. Water Sci. Technol. Water Supply 4, 155–

561   163. https://doi.org/10.2166/ws.2004.0073

562   Matsui, Y., Nakao, S., Sakamoto, A., Taniguchi, T., Pan, L., Matsushita, T., Shirasaki,

563   N., 2015. Adsorption capacities of activated carbons for geosmin and 2-

564   methylisoborneol vary with activated carbon particle size: Effects of adsorbent and

565   adsorbate characteristics. Water Res. 85, 95–102.

566   https://doi.org/10.1016/j.watres.2015.08.017

567   Matsui, Y., Nakao, S., Taniguchi, T., Matsushita, T., 2013b. Geosmin and 2-

568   methylisoborneol removal using superfine powdered activated carbon: Shell

569   adsorption and branched-pore kinetic model analysis and optimal particle size.

570   Water Res. 47, 2873–2880. https://doi.org/10.1016/j.watres.2013.02.046

571   Matsui, Y., Shirasaki, N., Yamaguchi, T., Kondo, K., Machida, K., Fukuura, T.,

572   Matsushita, T., 2017. Characteristics and components of poly-aluminum chloride

573   coagulants that enhance arsenate removal by coagulation: Detailed analysis of

574   aluminum species. Water Res. 118, 177–186.

575   https://doi.org/10.1016/j.watres.2017.04.037

576   Matsui, Y., Yoshida, T., Nakao, S., Knappe, D.R.U., Matsushita, T., 2012.

577   Characteristics of competitive adsorption between 2-methylisoborneol and natural

578   organic matter on superfine and conventionally sized powdered activated carbons.

579   Water Res. 46, 4741–4749. https://doi.org/10.1016/j.watres.2012.06.002

580   Nakamura, H., 2009. FT-NMR data processing by computer, Secong edi. ed. Sankyo

581   Shuppan.

582   Nakazawa, Y., Matsui, Y., Hanamura, Y., Shinno, K., Shirasaki, N., Matsushita, T.,

583   2018a. Minimizing residual black particles in sand filtrate when applying super-

584   fine powdered activated carbon: Coagulants and coagulation conditions. Water

585   Res. 147, 311–320. https://doi.org/10.1016/j.watres.2018.10.008

586   Nakazawa, Y., Matsui, Y., Hanamura, Y., Shinno, K., Shirasaki, N., Matsushita, T.,

587   2018b. Identifying, counting, and characterizing superfine activated-carbon

588   particles remaining after coagulation, sedimentation, and sand filtration. Water

589   Res. 138, 160–168. https://doi.org/10.1016/j.watres.2018.03.046

590   Pan, L., Nishimura, Y., Takaesu, H., Matsui, Y., Matsushita, T., Shirasaki, N., 2017.

591   Effects of decreasing activated carbon particle diameter from 30 Mm to 140 nm on

592   equilibrium adsorption capacity. Water Res. 124, 425–434.

593   https://doi.org/10.1016/j.watres.2017.07.075

594   Parker, D.R., Bertsch, P.M., 1992. Identification and Quantification of the "Al13"

595   Tridecameric Aluminum Polycation Using Ferron. Environ. Sci. Technol. 26, 908–

596   914. https://doi.org/10.1021/es00029a006

597   Partlan, E., Davis, K., Ren, Y., Apul, O.G., Mefford, O.T., Karanfil, T., Ladner, D.A.,

598   2016. Effect of bead milling on chemical and physical characteristics of activated

599   carbons pulverized to superfine sizes. Water Res. 89, 161–170.

600   https://doi.org/10.1016/j.watres.2015.11.041

601   Sato, F., Matsuda, S., 2009. Novel Basic Aluminum Chloride, Its Manufacturing

602   Method and Its Application. Japanese Patent, Appl.

603   Sposito, G., 1995. The Environmental Chemistry of Aluminum, Second Edition. Taylor

604   & Francis.

605   Sricharoenchaikit, P., Letterman, R.D., 1987. EFFECT OF AL(III) AND SULFATE

606   ION ON FLOCCULATION KINETICS. J. Environ. Eng. -ASCE 113, 1120–1138.

607   https://doi.org/10.1061/(ASCE)0733-9372(1987)113:5(1120)

608   Tang, H., Xiao, F., Wang, D., 2015. Speciation, stability, and coagulation mechanisms

609   of hydroxyl aluminum clusters formed by PACl and alum: A critical review. Adv.

610   Colloid Interface Sci. 226, 78–85. https://doi.org/10.1016/j.cis.2015.09.002

611 Wang, D., Sun, W., Xu, Y., Tang, H., Gregory, J., 2004. Speciation stability of

612   inorganic polymer flocculant-PACl. Colloids Surfaces A Physicochem. Eng. Asp.

613   243, 1–10. https://doi.org/10.1016/j.colsurfa.2004.04.073

614 Wang, D., Tang, H., Gregory, J., 2002. Relative importance of charge neutralization and

615   precipitation on coagulation of kaolin with PACI: Effect of sulfate ion. Environ.

616   Sci. Technol. 36, 1815–1820. https://doi.org/10.1021/es001936a

617 Yan, M., Wang, D., Ni, J., Qu, J., Chow, C.W.K., Liu, H., 2008. Mechanism of natural

618   organic matter removal by polyaluminum chloride: Effect of coagulant particle size

619   and hydrolysis kinetics. Water Res. 42, 3361–3370.

620   https://doi.org/10.1016/j.watres.2008.04.017

621 Yan, M., Wang, D., Qu, J., He, W., Chow, C.W.K., 2007. Relative importance of

622   hydrolyzed Al(III) species (Ala, Alb, and Alc) during coagulation with

623   polyaluminum chloride: A case study with the typical micro-polluted source

624   waters. J. Colloid Interface Sci. 316, 482–489.

625   https://doi.org/10.1016/j.jcis.2007.08.036

626 Ye, C., Wang, D., Shi, B., Yu, J., Qu, J., Edwards, M., Tang, H., 2007. Alkalinity effect

627   of coagulation with polyaluminum chlorides: Role of electrostatic patch. Colloids

628   Surfaces A Physicochem. Eng. Asp. 294, 163–173.

629   https://doi.org/10.1016/j.colsurfa.2006.08.005

630

Table 1

Ion components, alkalinity, and DOC of waters used in this study.

Series	Water	Na$^+$	K$^+$	Mg^{2+}	Ca^{2+}	Cl$^-$	NO$_3^-$	SO$_4^{2-}$	Alkalinity	DOC	Source
		mg/L	mg/L	mg/L	mg/L	mg/L	mg/L	mg/L	mg-CaCO$_3$/L	mg/L	
C Series	C0	13.8	1.7	4.5	5.8	11.9	0.3	18.8	27	2.4	Chibaberi River
	C1	33.0	1.7	4.3	5.7	14.4	0.0	15.9	50	0.9	
	C2	28.3	1.7	4.5	5.7	21.6	0.0	6.4	50	NM	
E Series	E1	24.2	0.6	0.0	12.5	22.5	0.9	0.0	50	NM	Elix water
	E2	24.1	0.5	0.6	12.3	22.1	0.9	3.5	50	NM	
	E3	24.0	0.6	1.3	12.5	22.3	1.0	6.4	50	NM	
	E4	25.3	0.5	3.9	12.5	25.7	1.1	15.8	50	NM	
	E5	30.5	0.6	0.0	12.5	22.1	0.9	15.7	50	NM	
	E6	20.5	0.5	6.1	12.3	25.3	1.0	28.2	50	NM	
	E7	21.0	0.5	10.2	12.3	25.7	1.0	48.8	50	NM	
J Series	J1	1.9	0.4	0.9	6.6	1.7	0.6	4.0	16	0.5	Joganji River
	J2	8.0	0.4	0.9	6.6	1.7	0.6	15.3	16	0.5	

(NM: Not measured, DOC: dissolved organic carbon)
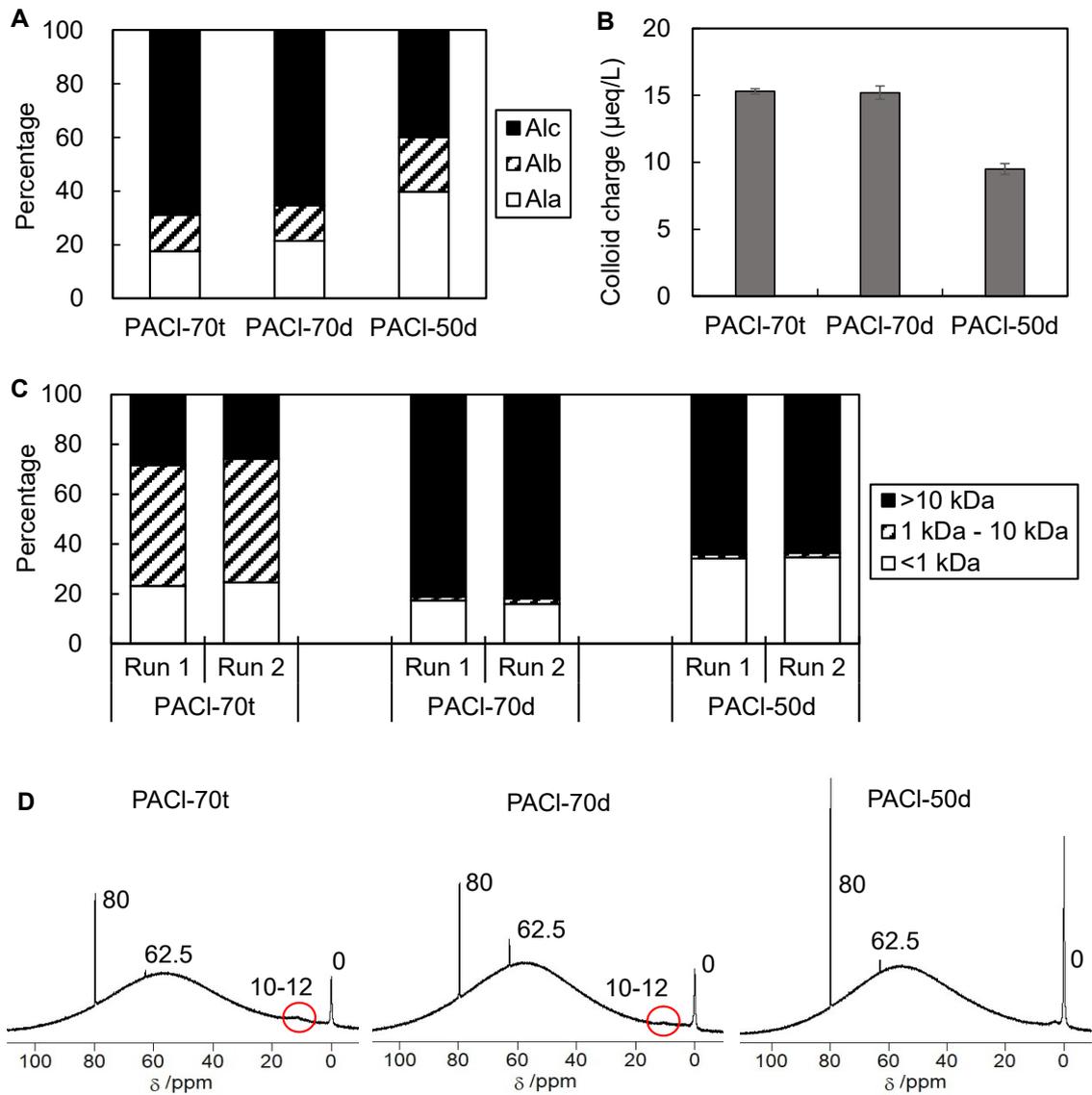
Fig. 1. Characteristics of PACl-70t, PACl-70d, and PACl-50d. Panel A: ferron distributions. Panel B: colloid charges. Panel C: molecular weight distribution of aluminum species (This experiment was conducted twice at the same condition. Panel D: of ^{27}Al-NMR spectra (The peaks at δ = 80 ppm are due to the internal standard, NaAl(OH)$_4$. The red circles indicate broad peaks at δ = 10-12 ppm).
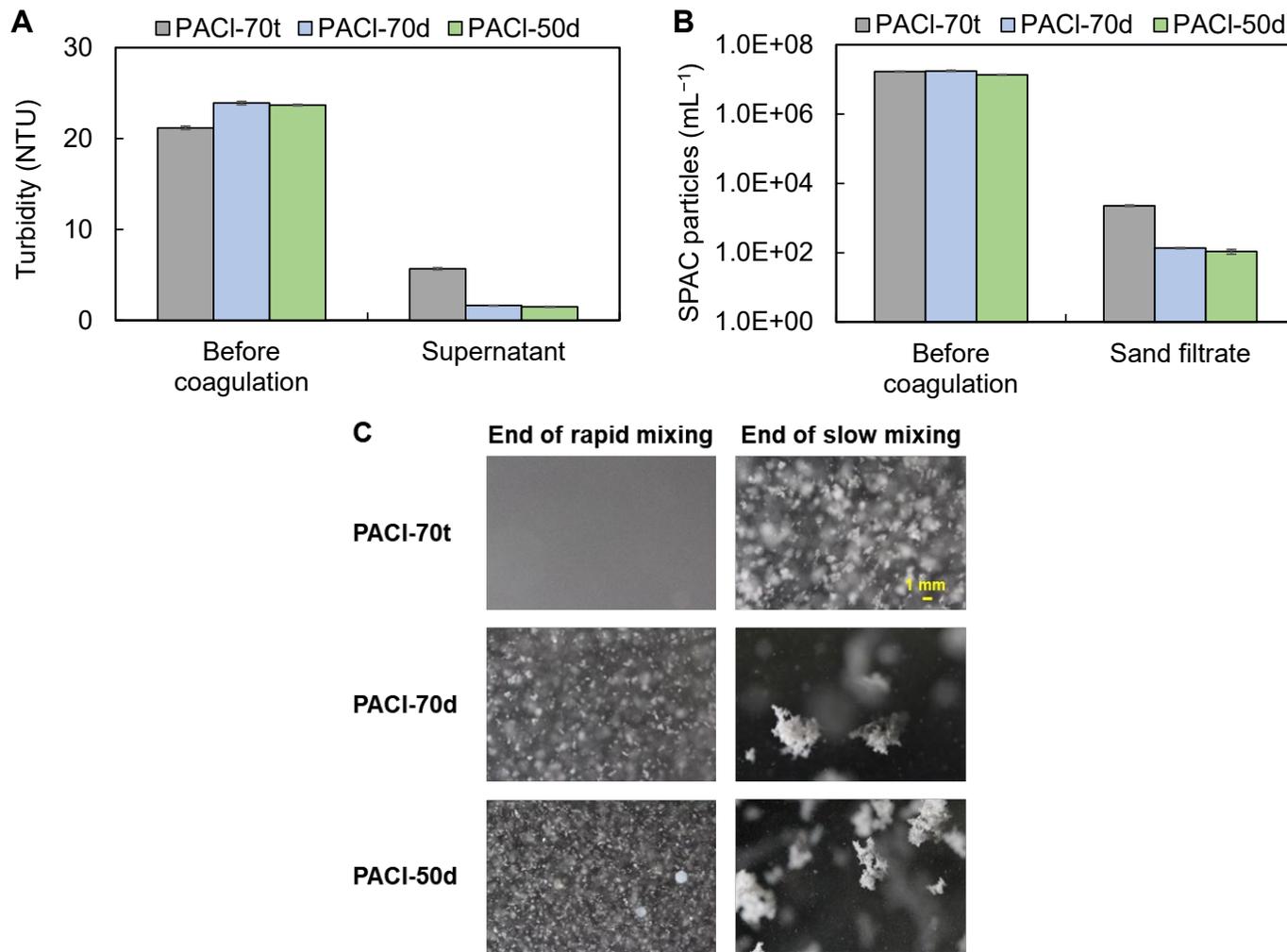
Fig. 2. Turbidity in supernatant (Panel A), residual SPAC particles in sand filtrate (Panel B), and photographs taken at the ends of rapid mixing and slow mixing (Panel C). Water C1 was used. Initial SPAC concentration was 2 mg/L. PACl-70t, PACl-70d, and PACl-50d were used at a dosage of 2.5 mg-Al/L. Coagulation pH was 7.0. Turbidities of sand filtrates were also measured, but they were very low: <0.1 NTU.
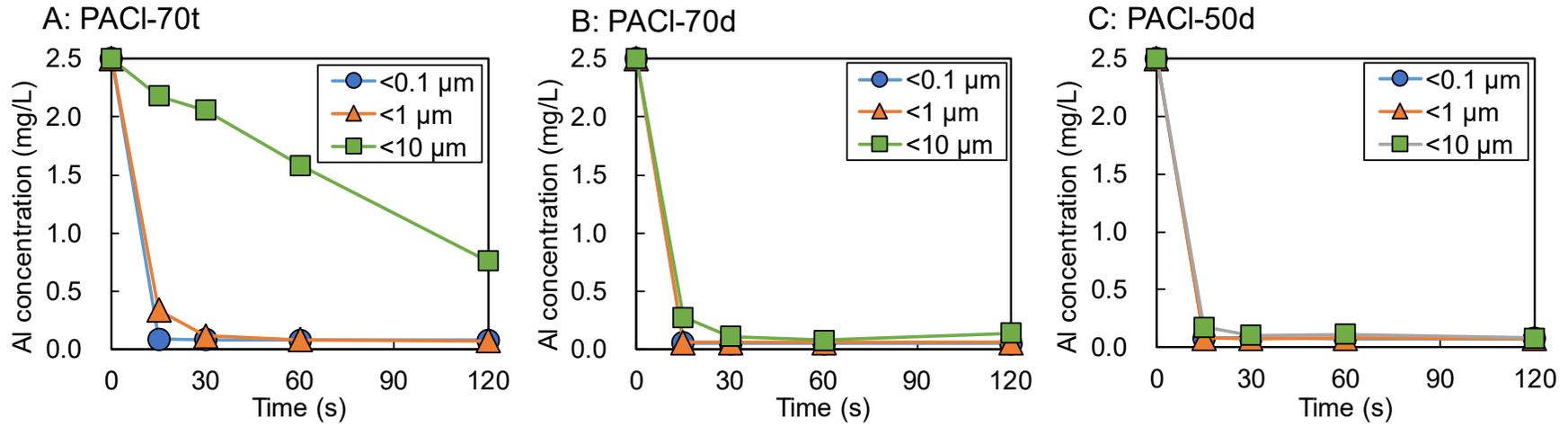
Fig. 3. Rate of hydrolysis of PACl-70t (Panel A), PACl-70d (Panel B), and PACl-50d (Panel C). Water E4 was used. PACl-70t, PACl-70d, and PACl-50d were used at a dosage of 2.5 mg-Al/L. Coagulation pH was 7.0.
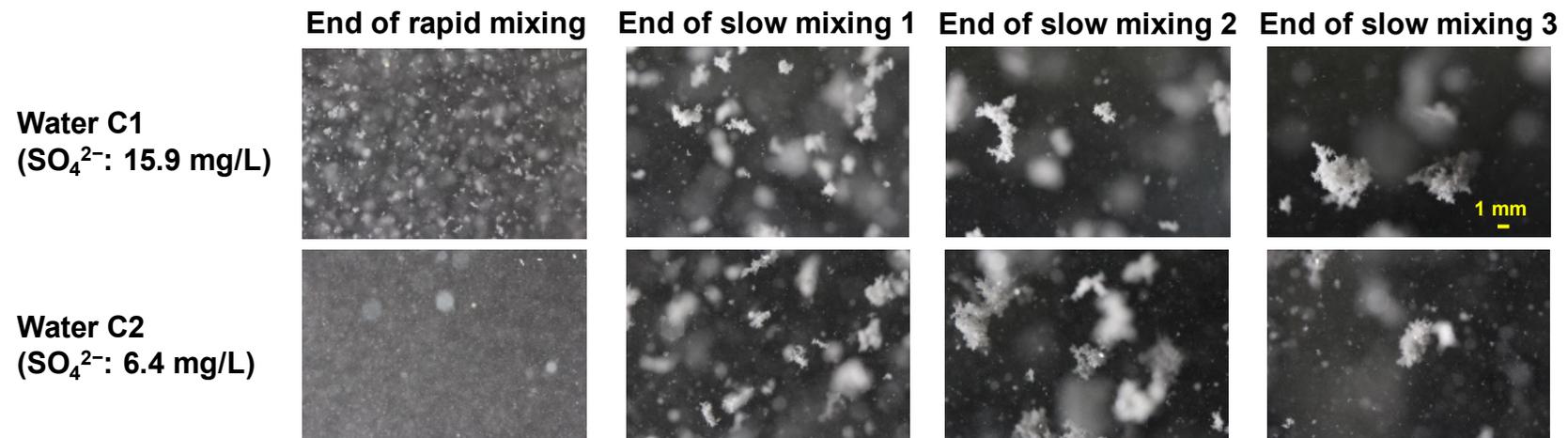
Fig. 4. Photographs taken at the end of rapid mixing and each slow mixing stage. Waters C1 (upper pictures) and C2 (lower pictures), including SO_4^{2-} concentrations of 15.9 and 6.4 mg/L, respectively, were used. Initial SPAC concentration was 2 mg/L. PACl-70d was used at a dosage of 2.5 mg-Al/L. Coagulation pH was 7.0.
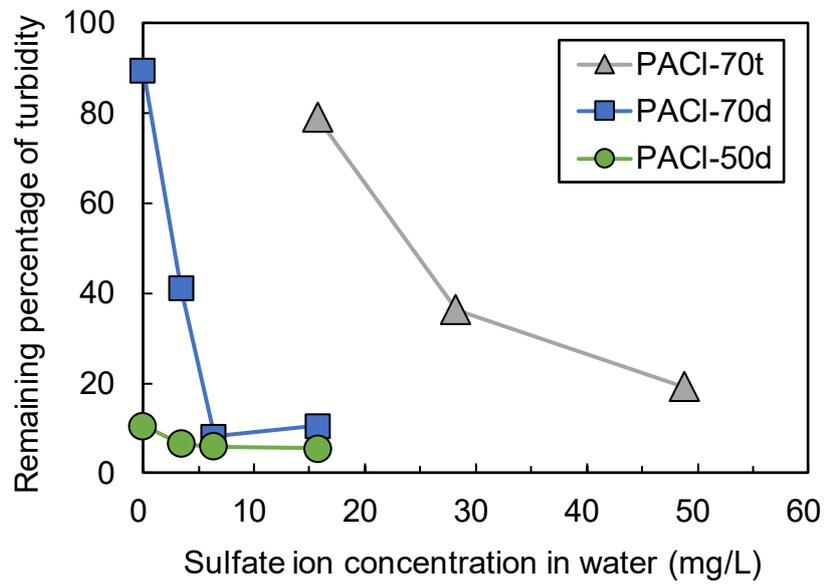
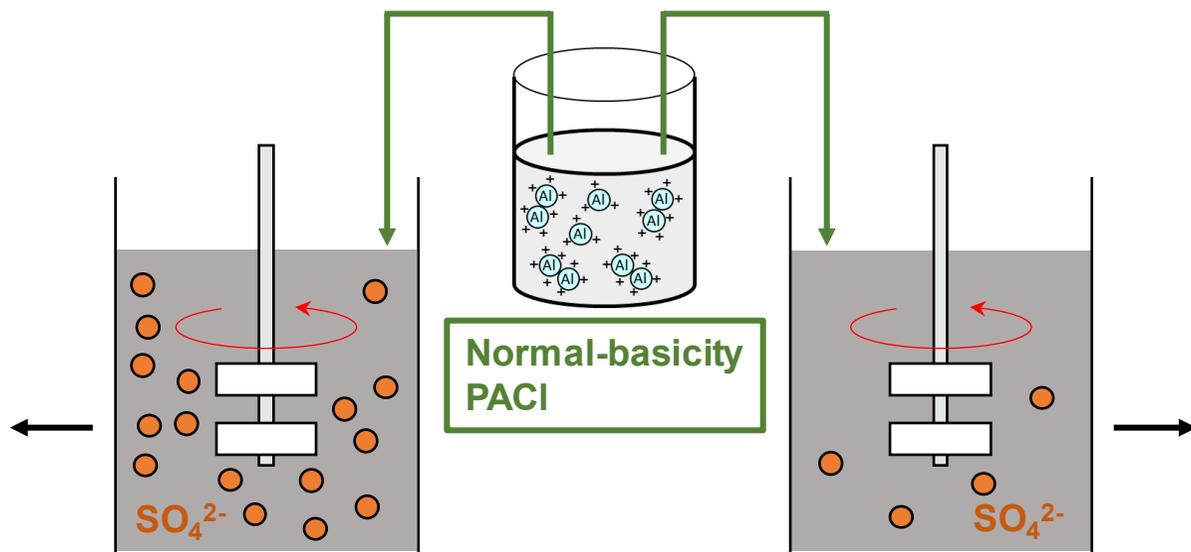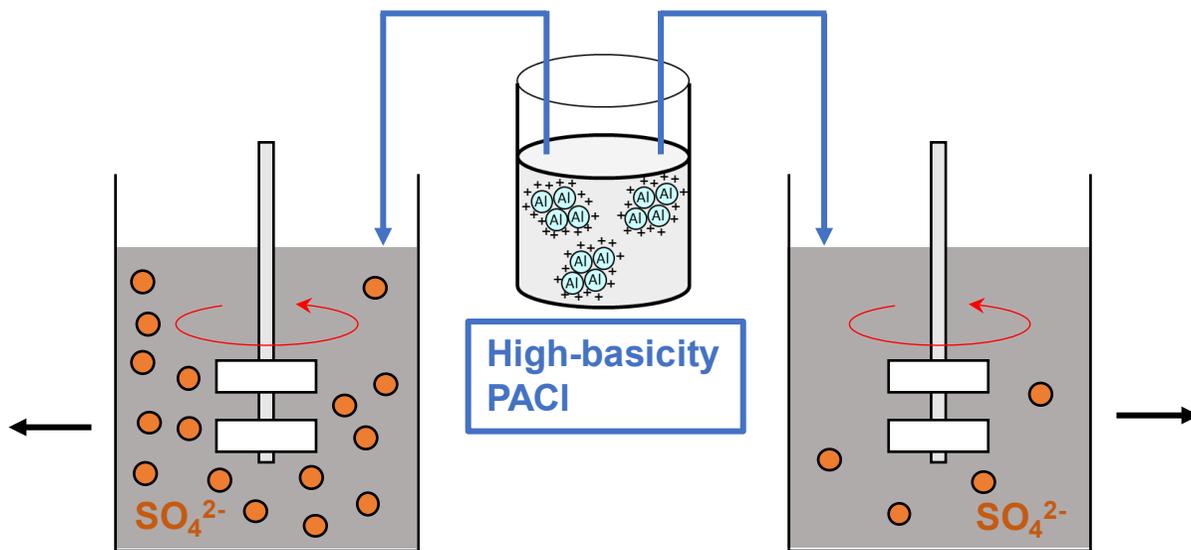**Fig. 5.** Plots of the percentage of turbidity remaining after coagulation and sedimentation against sulfate ion concentration in raw water. Waters E1–4 and E6-7 were used. Initial SPAC concentration was 2 mg/L. PACl-70t, PACl-70d, and PACl-50d were used at a dosage of 2.5 mg-Al/L. Coagulation pH was 7.0.
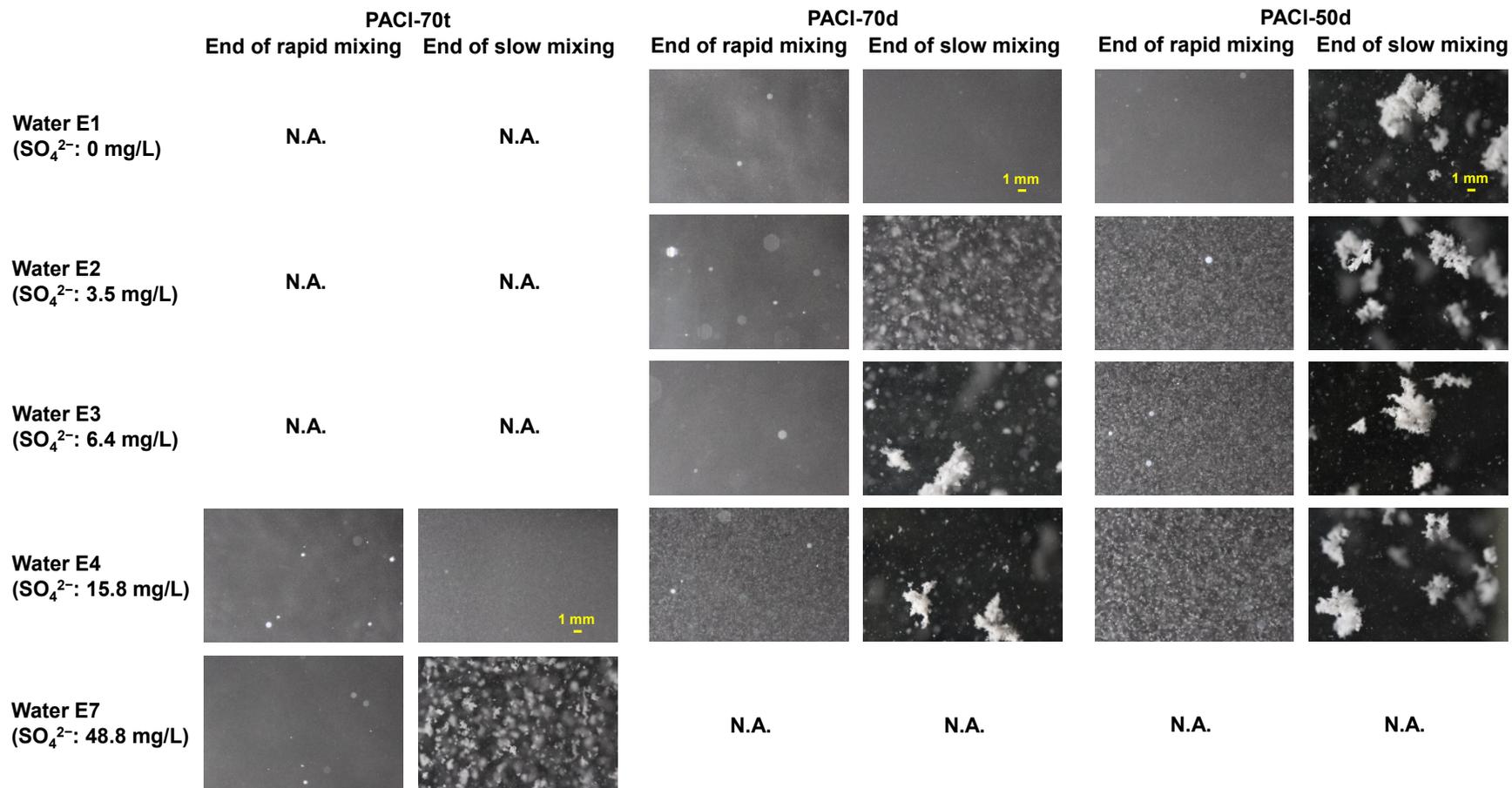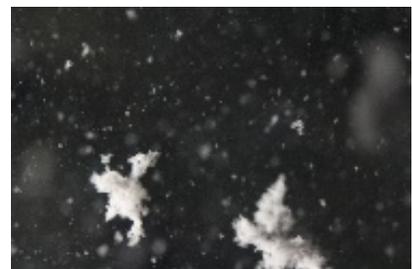
Fig. 6. Photographs taken at the end of slow mixing. Waters E1, 2, 3, 4, and 7 were used. Initial SPAC concentration was 2 mg/L. PACl-70t, PACl-70d, and PACl-50d were used at a dosage of 2.5 mg-Al/L. Coagulation pH was 7.0. All the pictures during slow mixing are shown in Fig. 6S, Fig. 7S, and Fig. 8S in the SI.
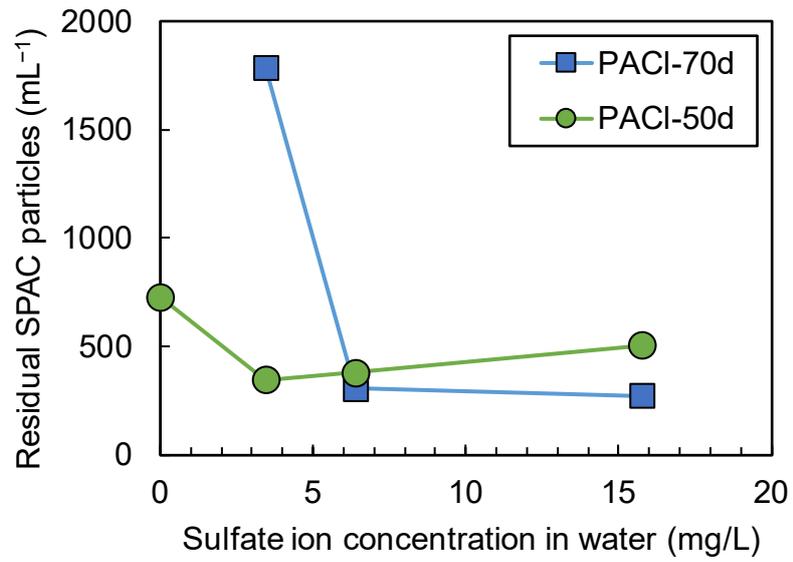
Fig. 7. Plots of residual SPAC particle concentration in sand filtrate against sulfate concentration in raw water. Waters E1, E2, E3, and E4 with sulfate ion concentrations of 0.0, 6.4, 15.8, and 28.2 mg/L, respectively, were used. Initial SPAC concentration was 2 mg/L. PACl dosage was 2.5 mg-Al/L. Coagulation pH was 7.0.
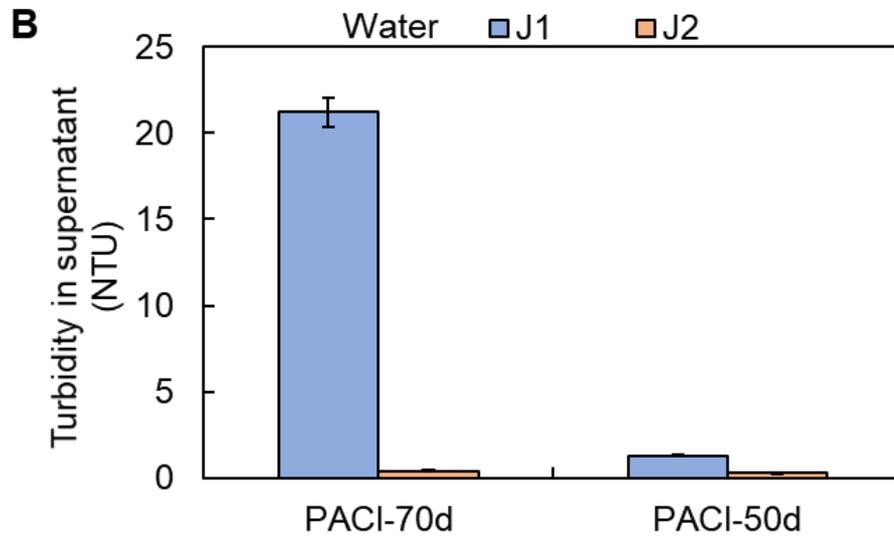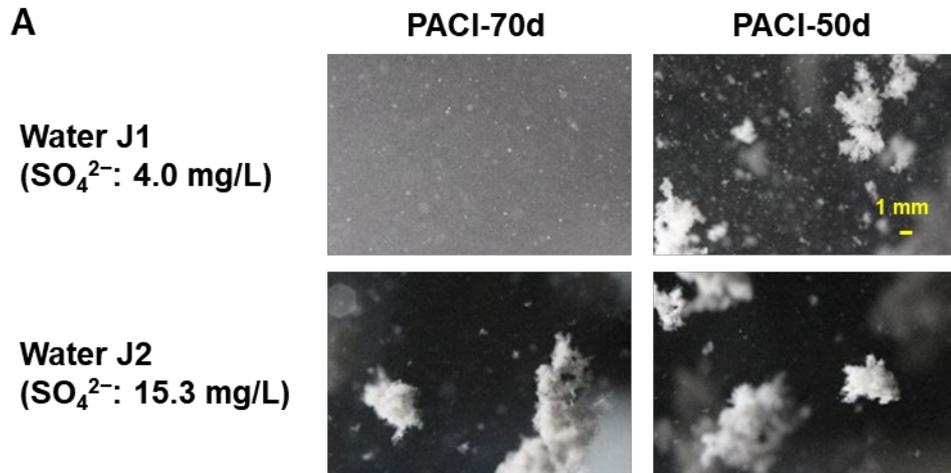
Fig. 8. Photographs taken at the end of slow mixing 3 (Panel A) and residual turbidities of supernatants (Panel B). Waters J1 and J2 with different sulfate ion concentrations of 4.0 and 15.3 mg/L, respectively, were used. Initial SPAC concentration was 2 mg/L. PACl-70d and PACl-50d were used at a dosage of 4.0 mg-Al/L. Coagulation pH was 7.0.

Fig. 9. Change of concentration of aluminum that passed through a membrane with a 10-µm pore size. Waters E1, E3, E4, E5, and E7 with sulfate ion concentrations of 0.0, 6.4, 15.8, 15.7, and 48.8 mg/L, respectively, were used. PACl-70t (Panel A), PACl-70d (Panel B), and PACl-50d (Panel C) were dosed at 2.5 mg-Al/L. pH during mixing was 7.

1

Highlights

- High-basicity PACl, esp. that made by $AlCl_3$-titration, is resistant to hydrolysis.

- $AlCl_3$-titration PACl is inferior to $Al(OH)_3$-dissolution PACl due to slow hydrolysis.

- Sulfate ions in raw water affect the performance of high-basicity PACl.

- High-basicity PACl requires sulfate ions, but normal-basicity PACl does not.

- Hydrolysis and charge neutralization capacity are both needed for coagulation.

8

High-basicity PACl

Normal-basicity PACl

SO_4^{2-}

1

2

Supplementary Information

4

5

6 Sulfate ion in raw water affects performance of high-basicity PACl

7 coagulants produced by Al(OH)3 dissolution and base-titration: removal

8 of SPAC particles by coagulation-flocculation, sedimentation, and sand

9 filtration

10

11 Yize Chen [a], Yoshifumi Nakazawa [a], Yoshihiko Matsui [b, *], Nobutaka Shirasaki [b], Taku

12 Matsushita [b]

13

14 [a] Graduate School of Engineering, Hokkaido University.

15   N13W8 Sapporo 060-8628 Japan

16 [b] Faculty of Engineering, Hokkaido University

17   N13W8 Sapporo 060-8628 Japan

18

19 * Corresponding author. Phone: +81-11-706-7280.

20   *E-mail address:* matsui@eng.hokudai.ac.jp (Y. Matsui)

21

22

23

24

25

Table 1S

Properties of the PACls used in this study.

|	PACl-70t	PACl-70d	PACl-50d
Al content (mol/L)	0.1	2.5	2.5
SO_4^{2-}/Al (mole ratio)	0.11	0.11	0.14
Na^+/Al (mole ratio)	2.18	0.27	0.00
Cl^-/Al (mole ratio)	3.86	1.04	1.25
Basicity (%)	69.6	68.1	50.6
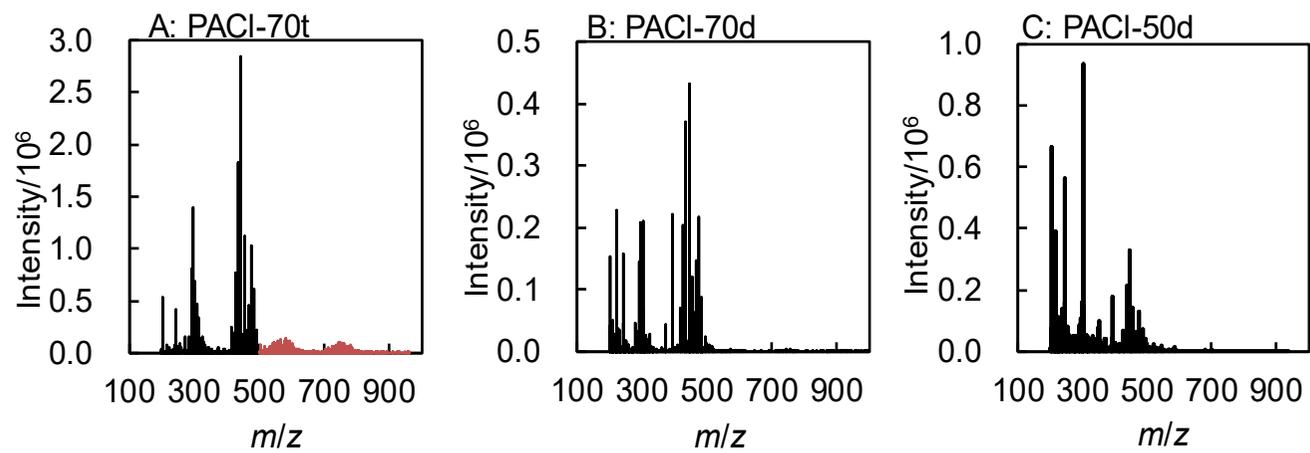
Fig. 1S. ESI-MS spectra of PACl-70t, PACl-70d, and PACl-50d.
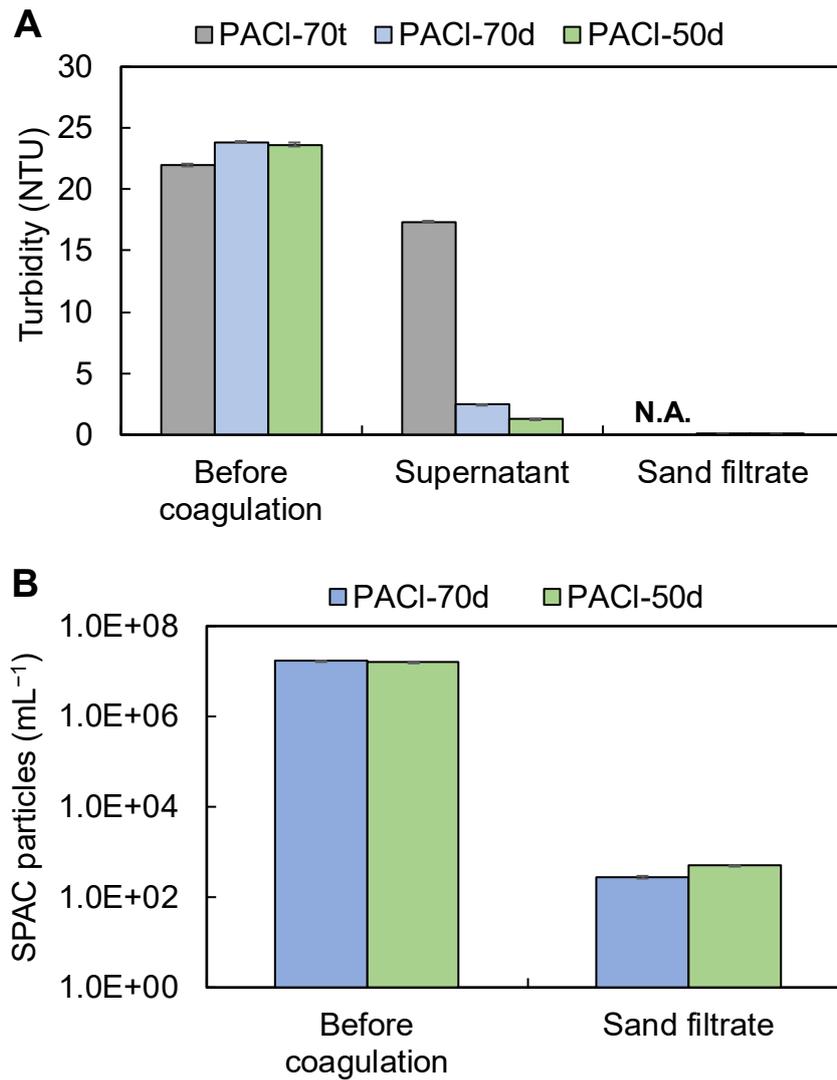
Fig. 2S. Turbidity in supernatant and sand filtrate (Panel A) and residual SPAC particles in sand filtrate (Panel B). Water E4 was used. Initial SPAC concentration was 2 mg/L. PACl-70t, PACl-70d, and PACl-50d were used with the dosage of 2.5 mg-Al/L. Coagulation pH was 7.0. The sand filtration was not conducted for PACl-70t, so the turbidity in sand filtrate of PACl-70t was not available (N.A.).
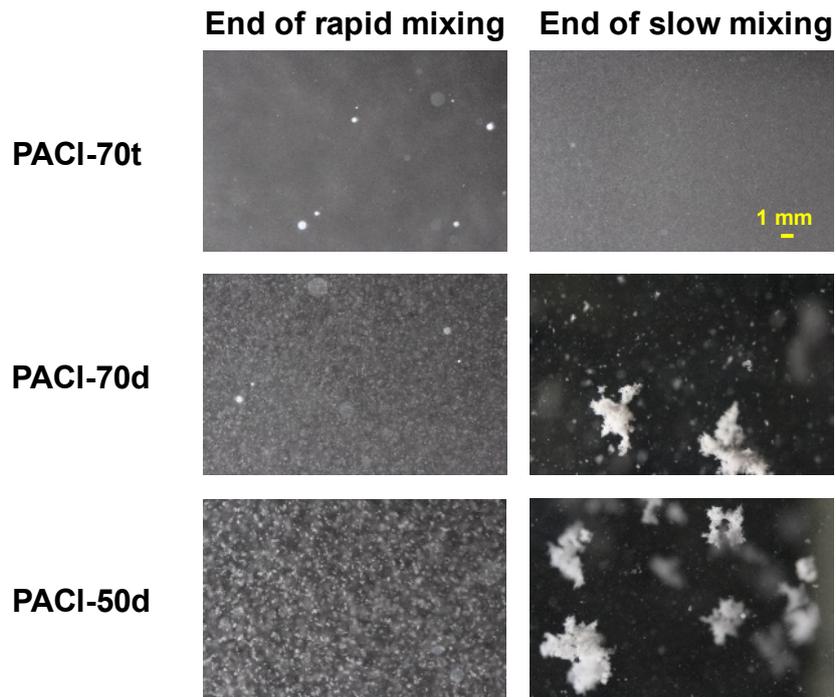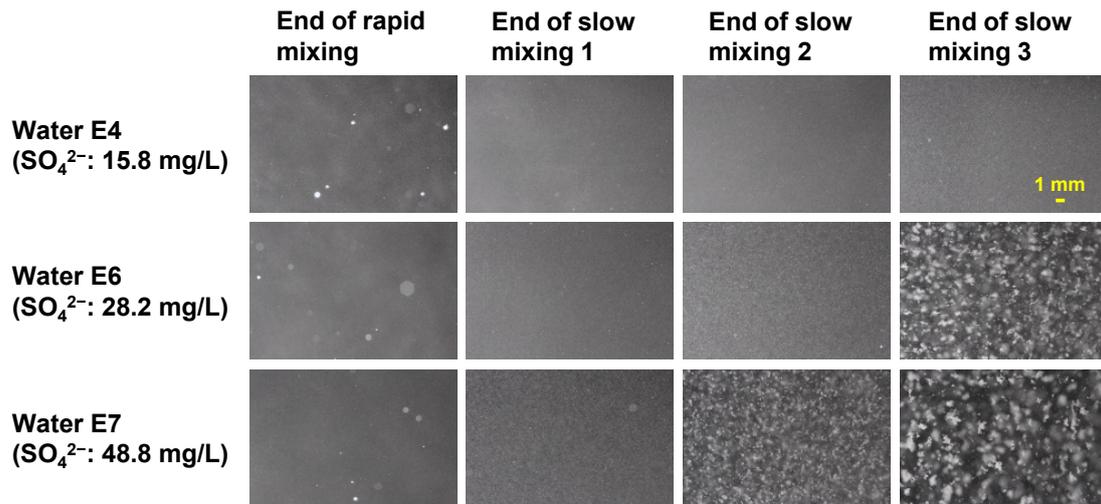
Fig. 3S. Photographs taken at the end of rapid mixing and slow mixing. Water E4 was used. Initial SPAC concentration was 2 mg/L. PACl-70t, PACl-70d, and PACl-50d were used at a dosage of 2.5 mg-Al/L. Coagulation pH was 7.0.
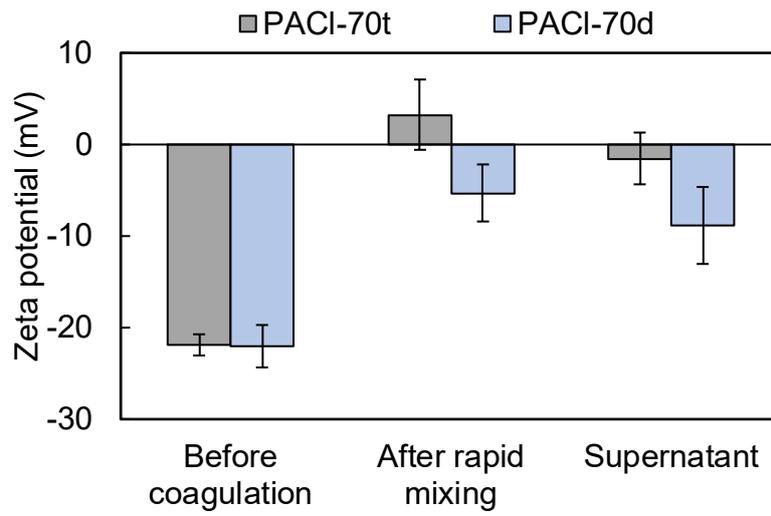
Fig. 4S. Change of zeta potential during CSF experiment. Water C1 was used. Initial SPAC concentration was 2 mg/L. PACl-70t and PACl-70d were used at a dosage of 2.5 mg-Al/L. Coagulation pH was 7.0.
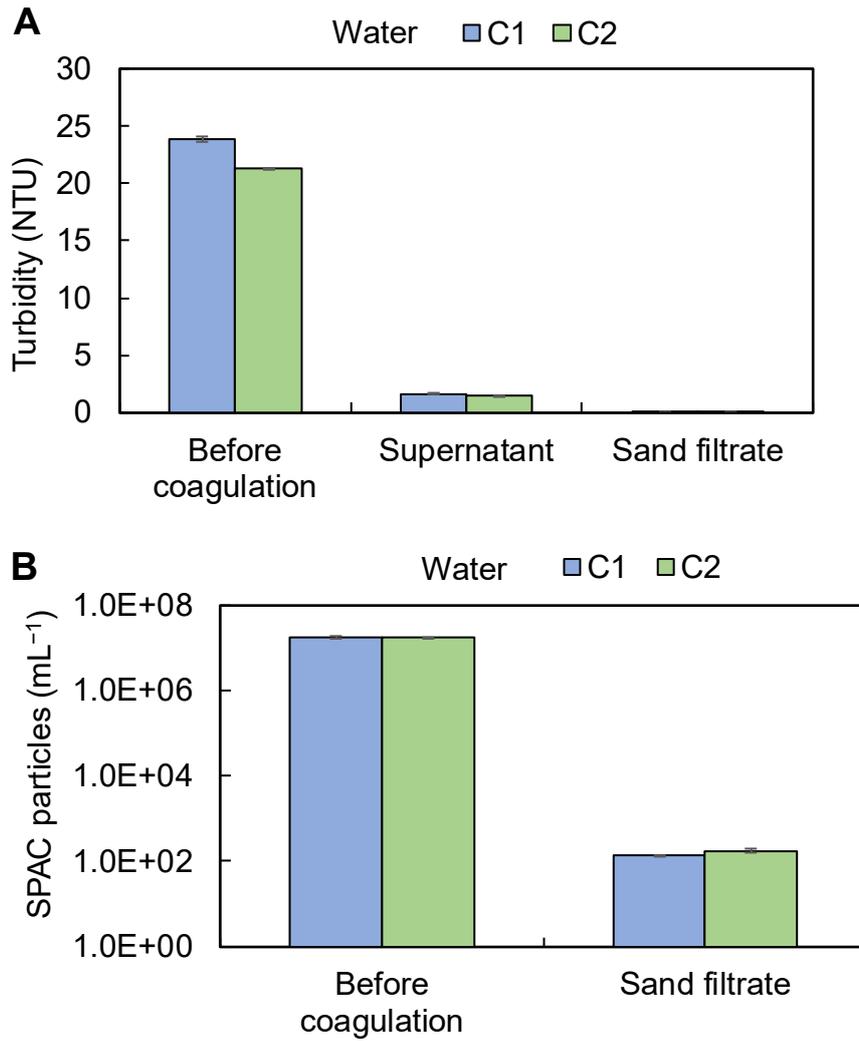
Fig. 5S. Changes of turbidity (Panel A) and SPAC-particle number concentration (Panel B) during CSF. Waters C1 (SO_4^{2-} 15.9 mg/L) and C2 (SO_4^{2-} 6.4 mg/L) were used. Initial SPAC concentration was 2 mg/L. PACl-70d was used at a dosage of 2.5 mg-Al/L. Coagulation pH was 7.0.

Fig. 6S. Photographs taken at the ends of rapid mixing, slow mixing 1, slow mixing 2, and slow mixing 3. Waters E4, E6 and E7 with sulfate ion concentrations of 15.8, 28.2, and 48.8 mg/L, respectively, were used. Initial SPAC concentration was 2 mg/L. PACl-70t was used at a dosage of 2.5 mg-Al/L. Coagulation pH was 7.0.
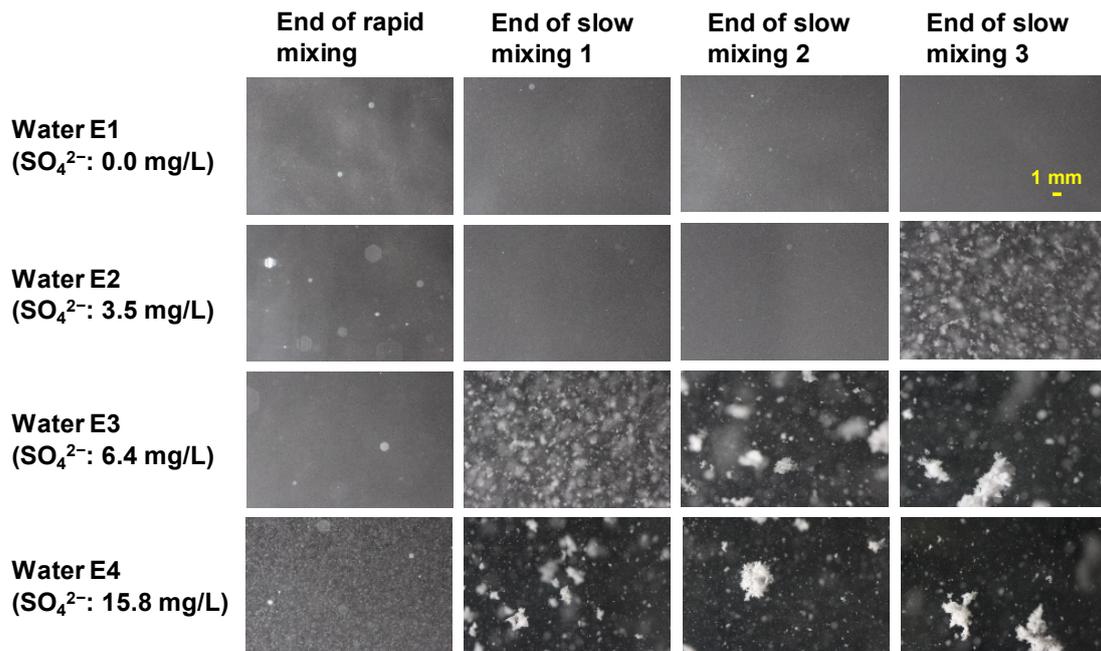
Fig. 7S. Photographs taken at the end of rapid mixing, slow mixing 1, slow mixing 2, and slow mixing 3. Waters E1, E2, E3, and E4 with sulfate ion concentrations of 0.0, 3.5, 6.4 and 15.8 mg/L, respectively, were used. Initial SPAC concentration was 2 mg/L. PACl-70d was used at a dosage of 2.5 mg-Al/L. Coagulation pH was 7.0.
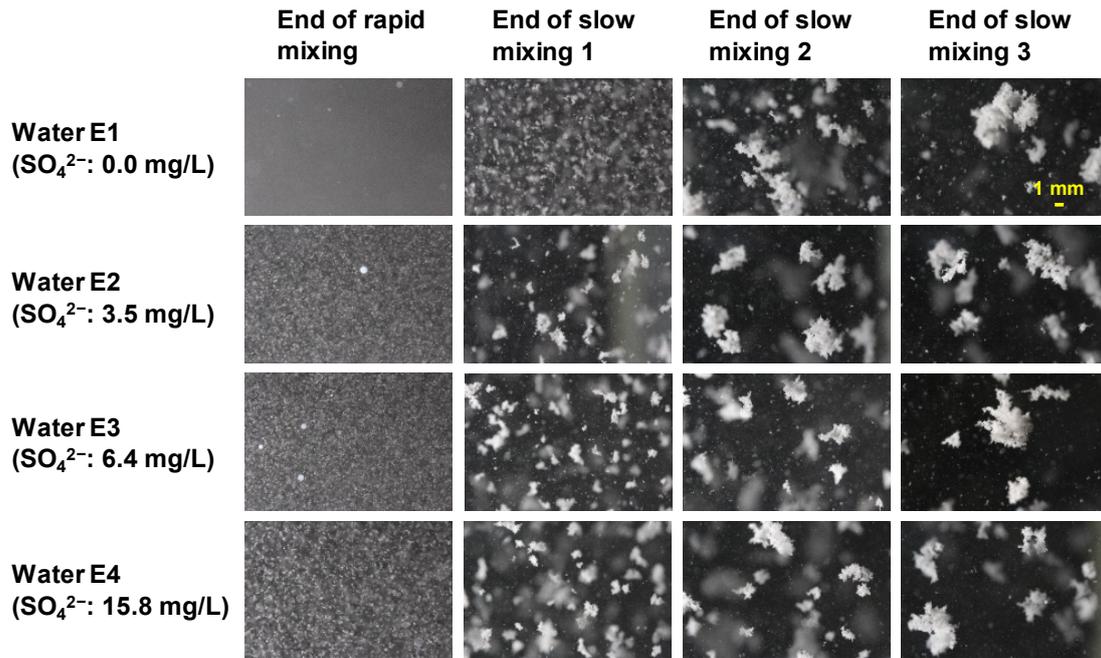
Fig. 8S. Photographs taken at the end of rapid mixing, slow mixing 1, slow mixing 2, and slow mixing 3. Waters E1, E2, E3, and E4 with sulfate ion concentrations of 0.0, 3.5, 6.4 and 15.8 mg/L, respectively, were used. Initial SPAC concentration was 2 mg/L. PACl-50d was used at a dosage of 2.5 mg-Al/L. Coagulation pH was 7.0.
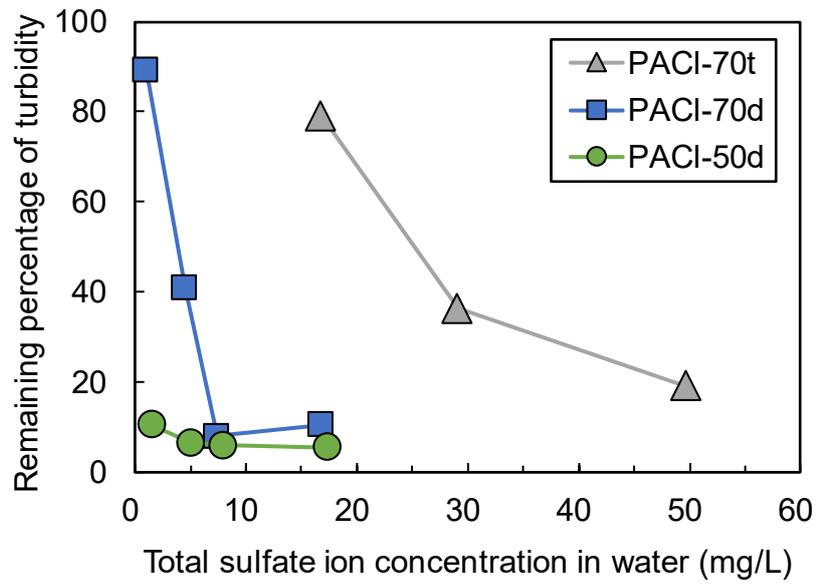
Fig. 9S. Plots of the percentage of turbidity remaining after coagulation and sedimentation against total sulfate ion concentration in raw water. Waters E1–4, and E6–7 with different sulfate ions were used. Initial SPAC concentration was 2 mg/L. PACl-70t, PACl-70d, and PACl-50d were used at a dosage of 2.5 mg-Al/L. Coagulation pH was 7.0.